5th International Conference on Durability of Concrete Structures
Jun 30–Jul 1, 2016
Shenzhen University, Shenzhen, Guangdong Province, P.R.China

Progress of Carbonation in Chloride Contaminated Concretes

Y. C. Wang
School of Civil Engineering, Shenzhen University; Guangdong Provincial Key Laboratory of Durability for Marine Civil Engineering, Shenzhen, P.R.China

P. A. M. Basheer
School of Civil Engineering, University of Leeds, England, UK

S. Nanukuttan
School of Planning, Architecture and Civil Engineering, Queen's University Belfast, Northern Ireland, UK

Y. Bai
School of Civil, Environmental and Geomatic Engineering, London, the UK

ABSTRACT

Concretes used in marine environment are generally under the cyclic effect of CO_2 and chloride ions (Cl^-). To date, the influence of carbonation on ingress of chloride ions in concretes has been widely studied; in comparison, study on the influence of Cl^- on the progress of carbonation is limited. During the study, concretes were exposed to independent and combined mechanisms of carbonation and chloride ingress regimes. Profiles of apparent pH and chloride concentration were used to indicate the progress of carbonation and ingress of Cl^- in concretes. From the apparent pH profile, a carbonation front and a carbonation boundary were characterized according to profile of consumed hydroxyl ions (OH^-). Results show that carbonation was significantly slowed down due to the existence of Cl^-, *viz.* the depth of carbonation boundary was decreased; the profile of consumed OH^- became modest; the carbonation front for different mixes presented slightly different trends. For the sound concretes, carbonation generated microcracks on concrete surface and increased permeation properties; for the chloride contaminated concretes, due to the limited extent of carbonation, permeation properties did not present obvious difference.

Keywords: combined mechanism, carbonation, chloride ions, alkalinity, permeation properties, relative humidity

1. INTRODUCTION

Durability of concrete structures is a worldwide important studying topic, and it significantly influences the service life of a structure. Regarding all the aspects of the durability issues, carbonation and chloride ingress are two processes that may lead to corrosion of reinforcement. In certain structures, such as those exposed to atmospheric zone in marine environment (Castro, Moreno, & Genesca, 2000; Mohammed, Hamada, & Yamaji, 2004; Moradian, Shekarchi, Aabdollah, & Alidadi, 2012; Song, Liu, Yi, Xu, & Ge, 2013; Zhao, Zhang, & Ming, 2013) concretes undergo influences from both the carbonation and chloride ingress simultaneously or in succession. The successional carbonation and chloride ingress process can also occur in structures that constructed in cold regions (Aveldano & Ortega, 2011), where rock salt is usually used in winter to melt ice and contains significant amount of chloride ions (Cl^-). There is some evidence that the corrosion of reinforcement is accelerated when it is under the simultaneous effect of carbonation and chloride ions (Moreno, Morris, Alvarez, & Duffó, 2004; Neville, 2011; Pakawat & Uomoto, 2005). Therefore, ingress of Cl^- and carbonation in cover concretes under the combined mechanism of exposure needs to be studied.

The combined ingress of CO_2 and Cl^- in concretes is a complicate process, both of which include physical transport of air molecules or ions and chemical reactions with cement hydration products. The individual progress of carbonation and ingress of Cl^- in concretes have been studied for decades and the mechanisms have been well established (Papadakis, 2000; Papadakis, Vayenas, & Fardis, 1991; Tang, 2008; Tang & Gulikers, 2007); by contrast, the combined ingress of CO_2 and Cl^- in concretes is much more complicate and the process and reactions mechanisms need further study.

Regarding the combined mechanisms of ingress of CO_2 and Cl^- in concrete, from one hand, it has been proved that carbonation influences the ingress of Cl- obviously. It can be summarised as follows: at the early stage of carbonation, densification of concrete due to the formation of $CaCO_3$ slows down the ingress of Cl^- (Xu, Wang, & Jin,

2011); the carbonation process decreases the chloride binding capacity of cement paste and promotes the chloride ingress in a certain extent (Dhir, El-Mohr, & Dyer, 1996; Nielsen, Herfort, & Geiker, 2005; Sandberg, 1999). With the progress of carbonation, microcracks may be formed on concrete surface and decrease the resistance of chloride ingress (Jin, Sun, & Li, 2008). In hydrated cement paste, it is believed that the produced minerals for the reaction of Cl^- with cement hydration product had relatively smaller increase in volume, comparing with those for the carbonation process. Therefore, it is believed that change in microstructure of hydrated cement paste under the influence of Cl^- is less obvious than those under the carbonation process. To date, knowledge on the influence of Cl^- in concretes on progress of carbonation is limited and the mechanism is still vague. Xu et al. (2011) studied the effect of chloride ions on the carbonation of concrete. Results showed that the existence of chloride ions obviously slowed down the carbonation rate, and the authors dedicated this phenomenon to two reasons: the density of the structure due to the reaction of chloride ions with the hydrated cement paste; blocking of the pores due to the crystallisation of chloride salts at the relatively low RH during the carbonation process. In this study, the authors did not eliminate the influence of water on the progress of carbonation. Samples after immersion in chloride solution were placed in the CO_2 environment without conditioning water content to the same extent with that for the individual carbonation study.

In this paper, a systematic study on progress of carbonation in well cured, and chloride contaminated concretes is reported. By comparing the consumption of OH^- and change in RH and permeation properties of concretes that exposed to independent carbonation and combined chloride ingress and carbonation regimes, the mechanism on the influence of Cl^- on progress of carbonation is established.

2. EXPERIMENTAL PROGRAMME

Details of the experimental programme of this study are summarised below:

2.1 Concrete mixes used in this study

Table 1 gives details of the concrete mixes and the mix proportions used in this study. All of the concrete mixes were designed for a w/b of 0.55 and the total binder content of 320 kg/m^3. These two parameters were selected according to BS EN 206 for concrete exposed to XC2, XD2, and XS2 environments and for an expected service life of 50 years. The final mix proportion as presented in Table 1 was slightly changed based on the yield equation. Three types of binder were used, *viz.* Portland cement (PC), Pulverised Fuel Ash (PFA), and Microsilica (MS). Based on the w/b and type of binder used, the three mixes are denoted as 0.55PC, 0.55PFA, and 0.55PFA + MS, respectively. A polycarboxylate-based superplasticiser was used to adjust workability of fresh concretes for a slump of 50–90 mm [S2 class in BS EN 206 (British Standard EN 206, 2000)].

2.2 Manufacture of samples

Fresh manufactured concretes were cast into three types of slab with Marine plywood moulds:

Slab (A): with the size 500 mm × 500 mm × 80 mm were cast for coring 75 mm diameter × 80 mm long cylindrical specimens, which were used to determine the extent of carbonation and distribution of chloride ions.

Slab (B): with the size 150 mm × 150 mm × 80 mm were used to obtain the distribution of RH in concretes during conditioning and carbonation processes. In each sample, four PVC pipes, with the length of 10, 20, 30, and 40 mm, were embedded. The schematic figure of the samples is shown in Figure 1. By measuring the RH of the formed PVC chambers, RH of concrete at the designated depths were obtained. The formed holes were sealed with rubber bungs between measurements, in order to prevent moisture movement.

Slab (C): with the size 230 mm × 230 mm × 80 mm were cast for detecting change in permeation properties of the concretes during the different exposure regimes.

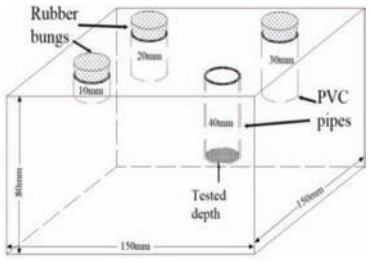

Figure 1. Schematic figure of slab for monitoring RH of concretes.

Table 1. Mix proportion of concretes.

		Quantities (kg/m^3)								
Mixes	**Binder content (%)**	**Cement**	**FA**	**SF**	**Sand**	**10 mm-Agg**	**20 mm-Agg**	**Superplasticiser**	**Water**	**w/b**
0.55PC	PC(100)	338	0	0	683	663	663	1.6	176	0.55
0.55PFA	PC(70) + PFA(30)	234	100	0	677	658	658	1.68	176	0.55
0.55PFA + MS	PC(85) + PFA(10) + MS(5)	285	34	17	679	659	659	2.18	176	0.55

2.3 Curing of samples

After the cast in marine plywood moulds, all the samples were then covered with a polythene sheet and were placed in a room at a temperature of 20 ± 2°C for 24 h. Subsequently, the samples were demoulded and experienced another period of 55 days of curing, including a period of water curing of the hardened concrete for 6 days at temperature of 20 ±1°C and storage in a room at temperature of 20 ± 1°C and RH of 55–65% for 49 days. After the curing, 16 cylindrical samples with a dimension of ϕ75 mm × 80 mm were extracted from the central part of each 500 mm × 500 mm × 80 mm slab.

2.4 Conditioning of samples for different exposure regimes

The concrete samples manufactured were divided into two groups equally. One group samples experienced individual effect of carbonation, which was denoted as "yCO_2." The other group samples experienced chloride ingress followed with carbonation and were denoted as "xCl^- + yCO_2." In the notations, "x" and "y" indicate the duration of immersion in chloride solution and carbonation, in months, respectively.

As water content in concretes significantly influences progress of carbonation, all the samples for studying carbonation were conditioned to a same consistence of RH of 65% state prior to been exposed to the CO_2 environment. Detailed procedures for conditioning of samples are as followed.

2.4.1 Conditioning of concrete for the individual carbonation (yCO_2)

2.4.1.1 Saturation of concrete samples

All the cast slab and cored cylindrical samples were covered with two layers of air and water proof acrylic paint (Sikagard 680) on the side surface, which ensured a uni-directional movement of water, air, and ions in the samples. After the paint had dried, the samples were placed on a wire mesh in a water tank with the mould finished surface facing downward. The samples were then saturated by means of an incremental water immersion method with duration of 9 days. At the end of the ninth day, samples were taken out from the water, and the trowel finished surface was painted immediately with the paint, leaving the mould finished surface uncovered and exposed to environment.

2.4.1.2 Oven drying of the concretes

The saturated samples were placed in a 40°C oven for water evaporation from the uncoated mould finished surface to decrease the water content. During this process, two slabs (B) for each mix were used to detect the water content in the concretes every 7 days. When moved out of the 40°C oven for the RH measurement, the concretes were immediately wrapped with polythene sheet to prohibit the absorption of moisture from environment and placed in a constant temperature room (20 ± 1°C). After about 24 h (almost cooling down to the room temperature), the RH at the exposure surface and the depths of 10, 20, 30, and 40 mm was measured with a capacity-based RH probe (Figure 2). If the average value of these measured depths was higher than 70%, the concretes were placed back in the over for a further 7-day drying. Once the value was at the range of 65–70%, the drying process was finished.

Figure 2. Measurement of the RH of concretes.

2.4.1.3 Redistribution of the inner moisture

The 40°C oven dried samples were sealed individually in air tight packages with polythene sheet and parcel tape and were placed in a 50°C oven to redistribute the inner RH. During this period, RH was measured every 2 weeks. If there was an obvious RH difference in concretes at the different measured depths, samples were sealed again and returned to the 50°C oven, until a consistence of RH of 65 ± 2% was achieved from the surface to the depth of 40 mm.

2.4.2 Conditioning of concrete for the chloride ingress followed with carbonation regime (xCl^- + yCO_2)

2.4.2.1 Saturation of concretes for the initial chloride ingress

Prior to been immersed in chloride solution for the initial chloride immersion stage, the side-coated samples were saturated following the procedures mentioned in Section 2.4.1.1.

2.4.2.2 Conditioning of concretes for the latter carbonation

After the chloride immersion stage, samples should retain its water saturation state. They were dried and redistributed the inner RH in ovens to achieve the consistence of RH of 65% state. Detailed procedures were the same as those presented in Sections 2.4.1.2 and 2.4.1.3.

2.5 Method of subjecting concretes to carbonation and chloride ingress

Carbonation of concretes was obtained by placing the conditioned RH of 65% concretes in a carbonation chamber with the set environment of 20°C, 5% CO_2, and 65% RH. For the chloride immersion stage

of the $xCl^- + yCO_2$ regime, the saturated samples were immersed in 165 g/l NaCl solution, and the NaCl tanks were placed in a temperature controlled room (20 ± 1°C). The duration of exposure for both carbonation and chloride ingress in the two combined carbonation and chloride ingress regimes was up to 3 months.

2.6 Tests carried out

2.6.1 Extraction of powder samples from cylindrical specimens

After been exposed to designated exposure regimes, two cylindrical specimens of each concrete mix were taken out for analysing the extent of deterioration. In each cylinder, powder samples were extracted from different depths of the cylinders with a profile grinder and the maximum depth was up to 35 mm. The exact depth where the powder samples were extracted from was measured with a vernier caliper at four different depths.

2.6.2 Determination of consumed OH^-, carbonated boundary, and carbonation front

Change in alkalinity of concrete during the exposure to the two regimes was determined by analysing the powder samples obtained. About 1 g (±0.001) powder was weighed and transferred to a 50-ml plastic bottle, and was mixed with 20 ml of deionised water. The bottle was tightly sealed and hand shaken for about 30 s. After 24 h standing, pH of the suspension samples was measured. The obtained pH value can indicate the alkalinity of concrete pore solution (Li, Sagüés, & Poor, 1999; McPolin, Basheer, Long, Grattan, & Sun, 2007; Sagüés, Moreno, & Andrade, 1997). As it is not the real pH of concrete pore solution, it was named as the apparent pH by McPolin et al. (2007).

Based on the basic chemical knowledge, the apparent pH is relevant to the concentration of corresponding OH^- in the suspension, following Eq. (1) (Li et al., 1999; Suryavanshi, Narayan, & Swamy, 1996). With the apparent pH result for concretes before exposing to the carbonation and chloride ingress regimes, the profiles of apparent pH in samples can be converted into the profiles of consumed OH^-. The relationship between the result of apparent pH and the amount of remaining and consumed OH^- is presented in Figure 3.

$$pH = 14 + \log([OH^-]) \quad (1)$$

As shown in Figure 4, based on the consumption of OH^-, a carbonated concrete can be divided into three regions, *viz.* the fully, partially, and none carbonated zones. In the fully carbonated zone, a further ingress of CO_2 will not lead to an obvious decrease in OH^- content; in the partially carbonated zone, there is a clear decrease of the consumed OH^- with depth. The boundary between these two zones was denoted as "X_b." In the non-carbonated zone, the OH^- had not reacted with CO_2. Therefore, the boundary between the partially and the non-carbonated zones indicates the front where the OH^- was starting to be consumed and was denoted as the "X_f."

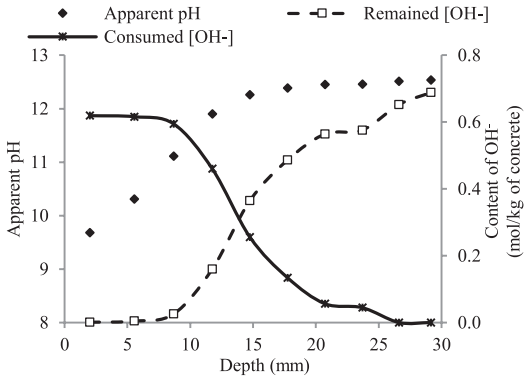

Figure 3. Relationship between apparent pH and remaining and consumed OH^- (specimen ID: 0.55PC 2.5CO_2).

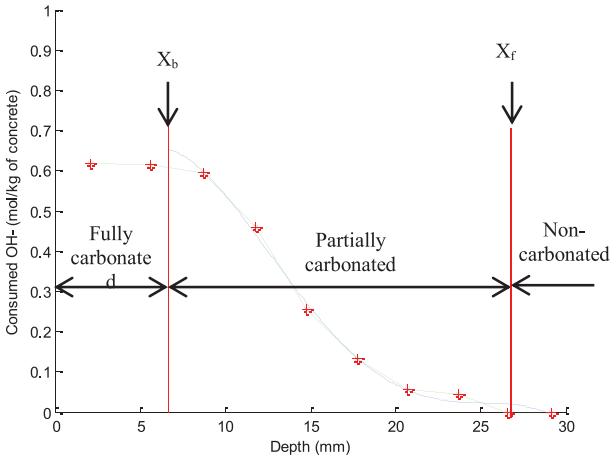

Figure 4. Analysis of the profile of consumed OH^- (specimen ID: 0.55PC 2.5CO_2).

As a known form of literature (Marchand, Bentz, Samson, & Maltais, 2001), during the immersion of concretes in chloride solution, calcium hydroxide will diffuse into solution, which also decreases the OH^- content. Therefore, in the "$xCl^- + yCO_2$" regime, the profile of consumed OH^- and the division of the three zones are related to both carbonation and chloride ingress. In this paper, to simplify the discussion, the X_b and X_f are named as the carbonation boundary and the carbonation front, regardless the reason for the OH^- variation.

2.6.3 Determination of chloride distribution

Acid-soluble chloride content in the samples was obtained by analysing the powder samples extracted and the procedures followed that recommended by RILEM (2002) (RILEM, 2002).

2.6.4 Determination of permeation properties of concretes

Change in permeation properties of concretes was detected on three 230 mm × 230 mm × 80 mm slabs by means of two on-surface devices, *viz.* the Autoclam Permeability System and the Permit Chloride Migration System. For each mix, the Autoclam, with the result of Air Permeability Index (API), was carried out every 2 weeks during the carbonation, while the Permit was carried out on two groups of three 230 mm × 230 mm × 80 mm slabs before and after the 3 months of carbonation for the change in steady-state migration coefficient (D_{SSM}). Prior to the Permit tests, the slabs were immersed in water for 1 week to get saturated with water.

2.6.5 Determination of RH of concretes

Change in RH of concrete during the carbonation stage of the individual and combined regimes was recorded every 2 weeks. Distribution of RH from concrete surface to the depth of 40 mm was tested with the RH probe on the two (B) slabs.

3. PRESENTATION AND DISCUSSION OF RESULTS

3.1 Progress of carbonation in concretes

3.1.1 Progress of carbonation in sound concretes

Figure 5(i) presents the consumed OH^- in the yCO_2 concretes. Correspondingly, the X_b and X_f are shown in Figure 5(ii). During the "yCO_2" regime, alkalinity of concrete was studied every 2 weeks. However, the profile of consumed OH^- was presented in a monthly basis in Figure 5(i) to keep the clarity of figures.

Before carbonation, the OH^- content of the three concretes was 0.62, 0.32, and 0.39 mol/kg of concrete, respectively. The relatively lower values in the 0.55PFA and the 0.55PFA + MS should be due to the use of PFA and MS, which consumed OH^- during their pozzolanic reaction. A higher OH^- content in the 0.55PFA + MS than that in the 0.55PFA should be mainly due to the lower substitution of cement in the 0.55PFA + MS (15%) than in the 0.55PFA (30%). In the profiles Figure 5(i), clearly show the progress of carbonation in concretes, which was the most obvious during the first month. Results of Figure 5(ii) show that the development of X_f in the three mixes was similar. However, in the aspect of X_b, the 0.55PFA had the highest value and that for the 0.55PC and the 0.55PFA + MS was close. Similar results on concrete alkalinity during carbonation were reported in other studies (McPolin et al., 2007; Sisomphon & Franke, 2007). In the results reported by McPolin et al. (2007), the PC concrete (w/b = 0.50) had a higher initial apparent pH value (and hence higher OH^- content) than the PFA and the MS concretes (w/b = 0.50); the carbonation rate in the PFA and the MS concretes was higher than that of the PC concrete. Therefore, it can be concluded that concretes with a comparatively high w/b, the individual use of PFA and MS will not improve the carbonation resistance.

It has been well established that there is a proportional relationship between the carbonation depth, tested with the phenolphthalein method, and the square root of the carbonation duration (Ho & Lewis, 1987; Sisomphon & Franke, 2007). During the analysis,

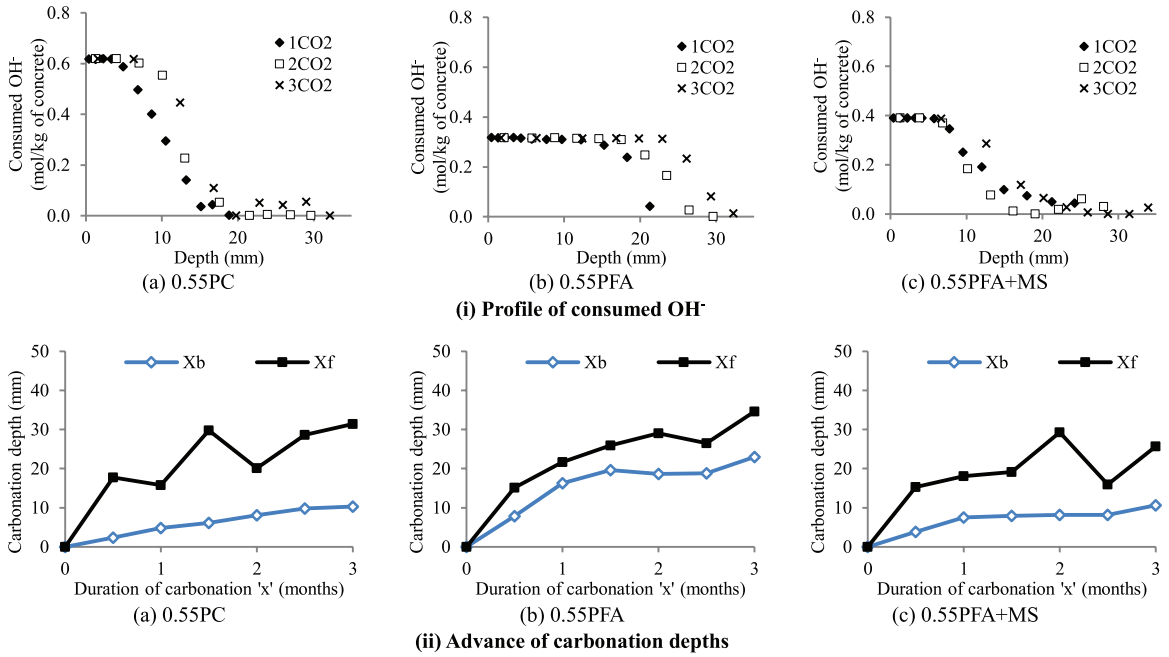

Figure 5. Progress of carbonation in concretes during the yCO_2 regime.

attempt was made to examine whether or not the X_b and X_f obtained from the apparent pH profile followed a similar relationship and the results are presented in Figure 6. The obtained results show that the relationships between the square root of the carbonation duration and the X_b and X_f are linear.

3.1.2 Progress of carbonation in chloride contaminated concretes

Figure 7 presents the progress of the consumed OH^- and the carbonation depths for concretes during the yCO_2 stage of the $3Cl^- + yCO_2$ regime. The profiles, shown in Figure 7(i), indicate that the consumption of OH^- at the surface layer mainly took place during the early stage of carbonation; at the late stage of carbonation, it mostly took place at deeper depths. Compared to the 0.55PC, the other two mixes, especially for the 0.55PFA, had a fully carbonated zone, which should be due to their relatively lower anti-carbonation property. The carbonation depths, as presented in Figure 7(ii), also show the progress of carbonation during the latter carbonation stage.

3.2 Change in RH of concrete during the carbonation stage

RH of concrete was monitored during the carbonation stage of the independent and the combined mechanisms. It was observed that for both of the two regimes studied the RH of the inner concrete (depths of 20, 30, and 40 mm) had similar values. Thus, an average RH value of the three depths is presented to indicate the RH condition of the inner concrete.

Figure 8 presents the change of RH during the $3CO_2$ process. Results showed that, in general, the RH decreased with the increase of the duration of the carbonation process. However, for the 0.55PFA concrete, the RH increased slightly at the initial

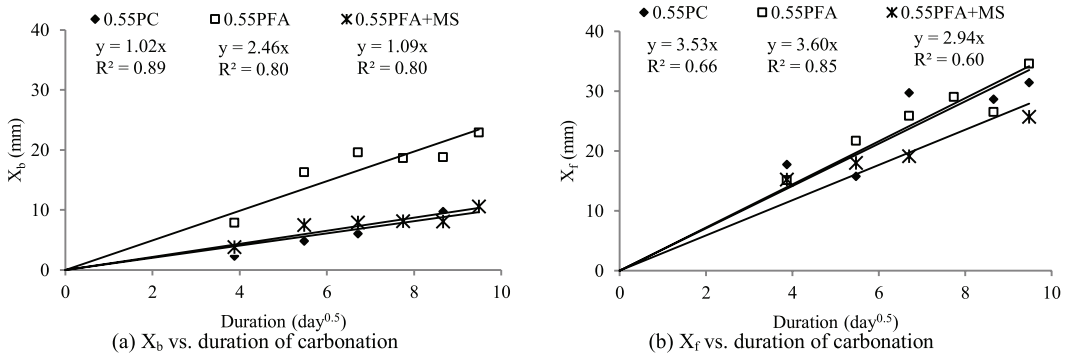

Figure 6. Relationship between the carbonation depths and the square root of duration of carbonation.

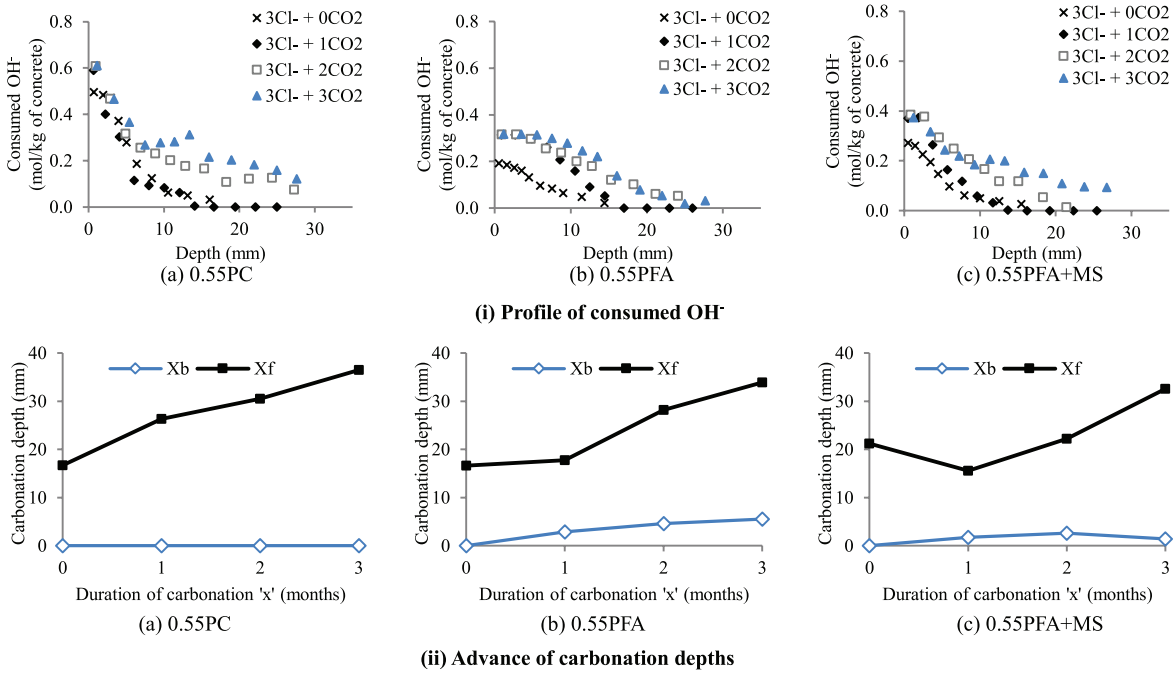

Figure 7. Variation of consumed OH^- in the concretes subjected to the $3Cl^- + yCO_2$ regime.

2 weeks. It was noticed that the initial RH of the 0.55PFA was in the range of 60–65%, which was slightly lower than that designated in the carbonation chamber (65%). Therefore, it can be assumed that the increase should be due to the absorption of water vapour by the concrete.

As water is generated during the carbonation, theoretically, carbonation of concrete should lead to an increase in RH. Russell (1999) studied the carbonation of concrete and reported the increase in RH at deeper parts of the concrete. The decrease in RH shown in Figure 8 might be due to the air circulation system employed in the carbonation chamber. In this project, air circulation of the carbonation chamber was used to maintain the consistent RH and temperature states. The air movement on the exposure surface of the samples led to a convection effect, which can continuously decrease the RH of the concrete (Af Klintberg & Björk, 2010; Choi, Cha, Oh, & Kim, 2011). The convection effect took place on the surface layer and led to the initial decrease of RH. Therefore, a RH gradient was formed and moisture from deeper parts of the concrete diffused to the surface, which should be the main reason for the RH decrease at the tested depths.

Figure 9 presents the development of RH in the $3CO_2$ stage of the $3Cl^- + 3CO_2$ regime. As seen from the results, prior to the carbonation, the RH values of the samples were conditioned to a range of about 60–70% (the RH of the 0.55PC at 0 and 10 mm and the 0.55PFA + MS at 0 mm were lower than 60%). After the 3 months of carbonation, the RH increased to the range of 68–75% and that of the surface layer was about 68–73%. The RH difference between the surface and the inner concrete decreased during the process.

The increase of RH could be due to the generation of water during the reaction of CO_2 with the cement hydration products and also from the decomposition of the Friedel's salt (Goni & Guerrero, 2003; Suryavanshi & Narayan Swamy, 1996). The chloride ions in the sample decreased the surface tension of the pore solution (Lide, 2004) and changed the relationship between the RH and the water content in the concrete. When the water content increased, the increase of RH in the chloride contaminated concrete was more obvious than that without the chloride ions. The influence of air circulation in the carbonation chamber on decreasing the RH of concrete, as observed in Figure 8 may be less significant, was not seen in these chloride contaminated samples.

3.3 Change in permeation properties of concretes

3.3.1 Air permeability index

Figure 10 presents change in the API during the 3 months of carbonation, and there was a general increase in the results for the mixes studied. In theory, the change in the API results during carbonation is related to a few parameters, including content of water, densification of concrete due to formation of $CaCO_3$, and formation of microcracks on concrete surface.

Theoretically, the content of water, which will be generated during carbonation, influences the permeation properties of concrete. During the $3CO_2$

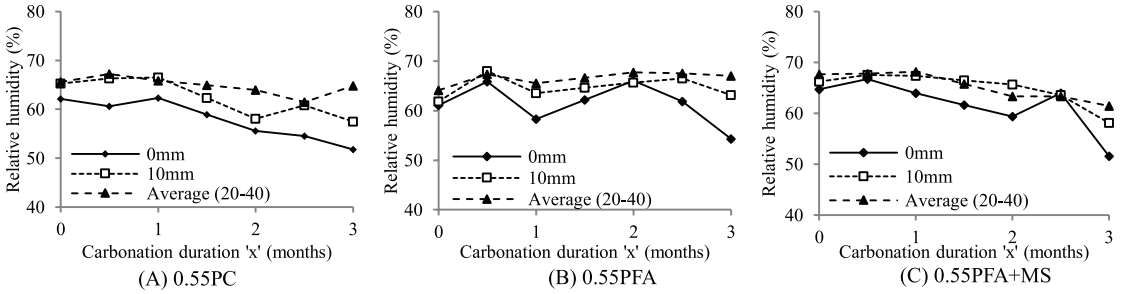

Figure 8. Change in RH during the $3CO_2$ stage of the $3Cl^- + 3CO_2$ regime.

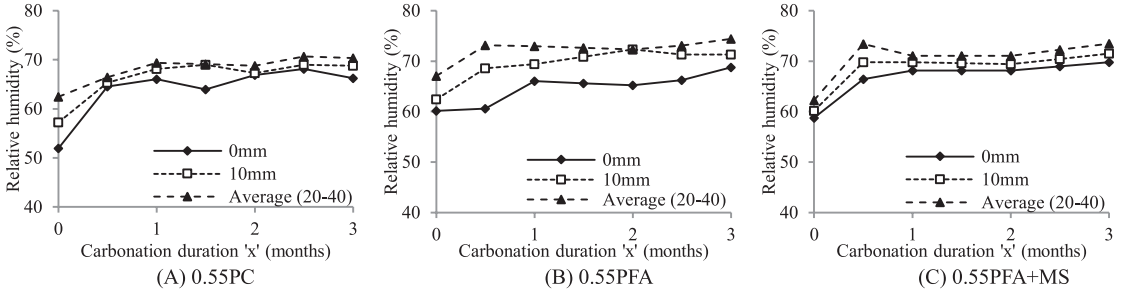

Figure 9. Change in RH during the $3CO_2$ stage of the $3Cl^-+3CO_2$ regime.

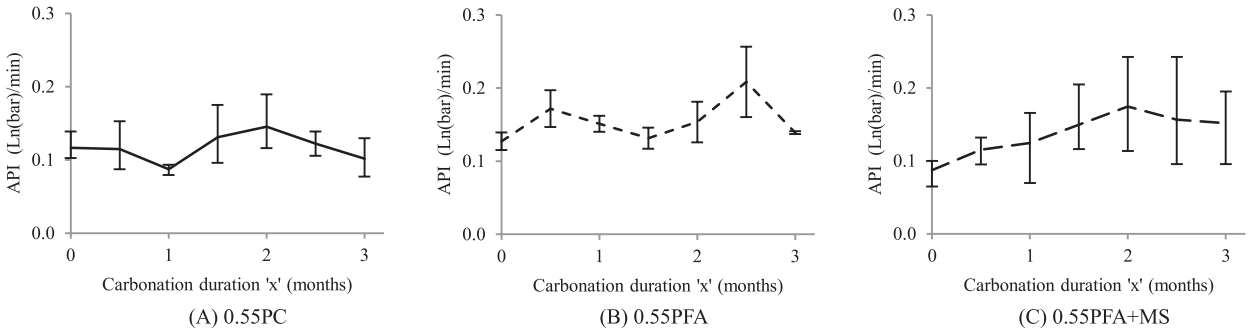

Figure 10. Change in API during the $3CO_2$ regime.

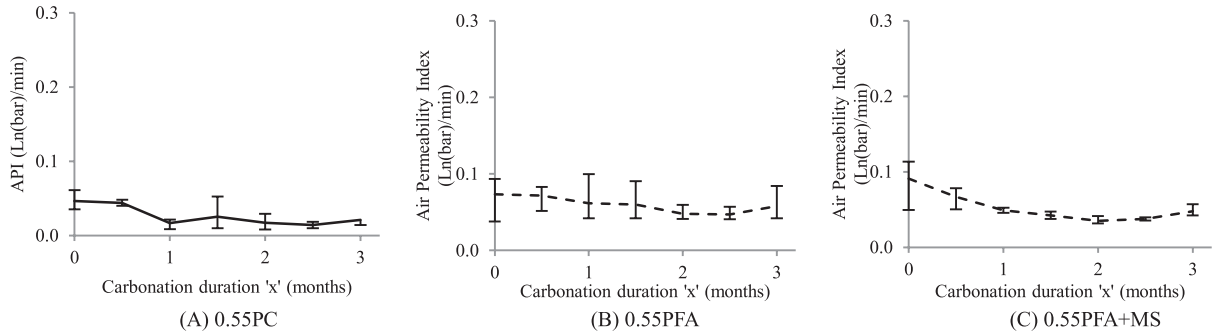

Figure 11. Change in API during the $3CO_2$ stage of the $3Cl^- + 3CO_2$ regime.

stage, the water content, in term of RH, at different depths of concrete was in a range of 50–70%, as reported in Figure 8, which have been proved lead to negligible influence on air permeability of concrete (Nolan, 1996; Parrott, 1991). Therefore, the change in the API in Figure 10 could be regarded as completely due to microstructure variation of concrete under carbonation. Based on existing knowledge, regarding the effect of carbonation, a decrease in API should be caused by formation of $CaCO_3$ from hydration products, which is a volume expansion process and densified the microstructure; an increase in values should be caused by the formation of cracks on concrete surface.

The observed increase in API for the three mixes is in consistent with findings reported in other studies on influence of carbonation on concretes: under the effect of carbonation, concretes with relatively higher w/b ratios are easily to get crack comparing with those with low w/b ratios (Ngala & Page, 1997); higher dosage of PFA increases the potential of cracking for concretes (Hobbs, 1994). Russell, Basheer, Rankin, and Long (2001) also studied changes in API of concretes under the effect of carbonation, and it was found that 15 out of 24 mixes presented an increasing trend and the rest mixes had almost constant API values. It can be assumed from the results obtained from this study and from Russell that the API for different concretes does not have any particular trend during carbonation. Therefore, in summary, the API is suit for qualitatively assessing changes in concrete permeability during carbonation, however, cannot accurately reveal the reactions taken place by itself.

3.3.2 Chloride migration coefficient

Figure 12 shows the D_{SSM} of concretes before and after the 3 months of carbonation stage in the two regimes. After the 56 days of curing, the D_{SSM} of the three mixes was in the range of 0.8 to 2.3 $\times$ 10^{-12} m^2/s and the values increased to about 12–15 times of their original values after the 3 months of carbonation. According to the analyses carried out in discussion on the API result, it can be concluded that the significant increase in the D_{SSM} value must be due to the cracks generated. In the $3Cl^- + 3CO_2$ regime, after the immersion of samples in NaCl solution for 3 months, the D_{SSM} results presented an noticeable increase, which should be because calcium hydroxide crystals leached out of the concrete and led to an increase in porosity at the surface layer (Marchand et al., 2001). During the 3 months of carbonation that followed the chloride immersion, the changes in the D_{SSM} was negligible comparing with that in the independent $3CO_2$ regime.

3.4 Effect of chloride ingress on carbonation of concrete

In Figures 5 and 7, the distribution of consumed OH^- and the carbonation depths in the concretes exposed to the yCO_2 and $3Cl^- + yCO_2$ regimes are presented. The differences show the influence of 3 months' immersion in chloride solution on carbonation of concrete. In the

$3Cl^- + yCO_2$ concretes, slop of the profiles in the region between X_b and X_f was more gentle than that of the yCO_2 concretes. The noticeable consumption of OH^- at deeper depths of the $3Cl^- + yCO_2$ concretes was likely to be due to the ionic exchange between Cl^- and OH^- during the previous chloride immersion stage.

Figure 13 presents comparison of the carbonation depths for concretes after the exposure to the two regimes. Figure 13(a) show that in the X_b of the $3Cl^- + yCO_2$ concretes had a comparatively lower value (0.55PFA and 0.55PFA + MS) or even disappeared (0.55PC). As due to the diffusion of calcium hydroxide into chloride solution, the amount of OH^- existed in the $3Cl^-$ concrete was relatively lower. In a subsequent yCO_2 stage, the consumed OH^- in the $3Cl^- + yCO_2$ concretes was substantially lower than that in yCO_2 concrete. This is considered to be due to the pore refinement of concrete as a result of chloride binding as mentioned previously. The 0.55PFA had the most obvious decrease in the X_b, which should be caused by its higher chloride binding capacity and a significant decrease in porosity after the binding. In comparison, the X_f fluctuated in the three mixes and the values for the carbonated concretes (those with the y of higher than 0) of the two regimes had no obvious difference.

4. CONCLUSION

In this paper, experimental work carried out in comparison progress of carbonation in well cured and chloride contaminated concretes was reported. To eliminate the influence of water on the carbonation process, samples were conditioned to the same consistence of RH of 65% state before been exposed to CO_2 environment. By testing different indicators in the two series of concretes, including consumption of OH^- and change in RH and indexes of permeation property, influence of Cl^- on progress of carbonation in the studied concretes was characterised. From the results and analyses as presented in this paper, it can be concluded that Cl^- in concretes can slow down the progress of carbonation. Detailed evidences those support this conclusion can be summarised as follows.

(1) In the previous chloride contaminated concrete, amount of OH^- consumed during carbonation was lower than those exposed to individual carbonation regime. Also, in the consumed OH^- profile, the gradient of the curve was relative modest and the carbonation boundary as determined decreased significantly.

(2) Under the exposure to the same CO_2 environment, the well-cured concrete had a decrease in RH. In comparison, those contained Cl^- had an increase in RH, which might hinder the transport of CO_2 molecules.

(3) Comprehensive results from the air permeability and the chloride migration tests proved the increase in permeation properties in concrete, which might be due to formation of microcracks.

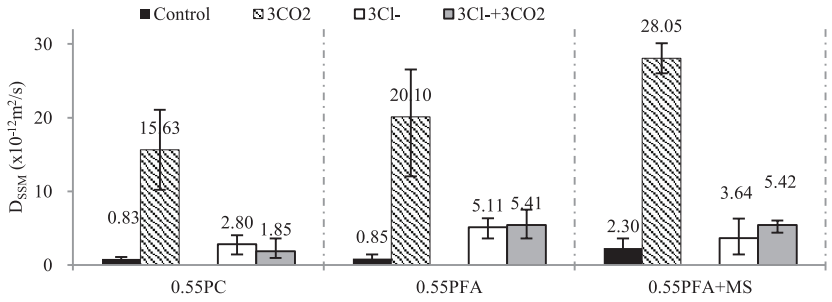

Figure 12. Change in D_{SSM} of the concretes.

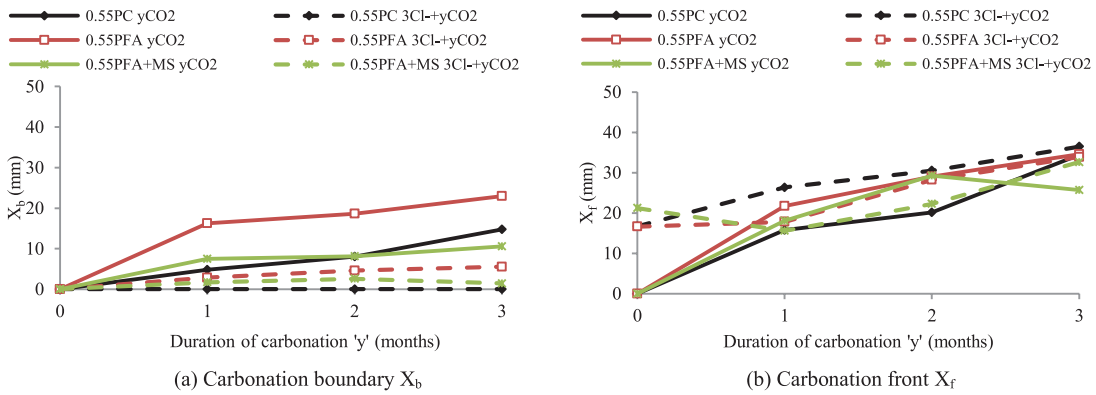

Figure 13. Comparison of X_b and X_f between the yCO_2 and $3Cl^- + yCO_2$ regimes.

For the carbonation after the chloride immersion stage, air permeability decreased and the chloride migration did not present obvious variation, which proved the densification of concrete, generally taken place at initial stage of carbonation.

ACKNOWLEDGMENTS

The authors gratefully acknowledge the financial support provided by the National Natural Science Foundation of China (No. 51408366 and No. 51520105012) and Shenzhen Government (JCYJ20150324141711682).

REFERENCES

Af Klintberg, T., & Björk, F. (2010). Air gap method: Drying of a concrete slab on ground construction. *Structural Survey, 28*(4), 281–299.

Aveldano, R. R., & Ortega, N. F. (2011). Characterization of concrete cracking due to corrosion of reinforcement in different environments. *Construction and Building Materials, 25*(2), 630–637.

British Standard EN 206. (2000). *Concrete – Part 1: Specification, performance, production and conformity*. London, England: British Standard Institution.

Castro, P., Moreno, E. I., & Genesca, J. (2000). Influence of marine micro-climates on carbonation of reinforced concrete building. *Cement and Concrete Research, 30*(10), 1565–1571.

Choi, S., Cha, S. W., Oh, B. H., & Kim, I. H. (2011). Thermo-hygro-mechanical behavior of early-age concrete deck in composite bridge under environmental loadings. Part 1: Temperature and relative humidity. *Materials and Structures, 44*(7), 1325–1346.

Dhir, R., El-Mohr, M. A. K., & Dyer, T. D. (1996). Chloride binding in GGBS concrete. *Cement and Concrete Research, 26*(12), 1767–1773.

Goni, S., & Guerrero, A. (2003). Accelerated carbonation of Friedel's salt in calcium aluminate cement paste. *Cement and Concrete Research, 33*(1), 21–26.

Ho, D., & Lewis, R. (1987). Carbonation of concrete and its prediction. *Cement and Concrete Research, 17*(3), 489–504.

Hobbs, D. (1994). Carbonation of concrete containing PFA. *Magazine of concrete research, 40*(143), 69–78.

Jin, Z. Q., Sun, W., & Li, Q. Y. (2008). Effect of carbonation on chloride diffusion in concrete. *Journal of University of Science and Technology Beijing, 30*(8), 921–925.

Li, L., Sagüés, A. A., & Poor, N. (1999). In situ. leaching investigation of pH and nitrite concentration in concrete pore solution. *Cement and Concrete Research, 29*(3), 315–321.

Lide, D. R. (2004). *CRC handbook of chemistry and physics 2004–2005: A ready-reference book of chemical and physical data*. CRC Press.

Marchand, J., Bentz, D. P., Samson, E., & Maltais, Y. (2001). Influence of calcium hydroxide dissolution on the transport properties of hydrated cement systems. In J. Skalny, J. Gebauer, & I. Odler (Eds.), *Materials science of concrete special volume: Calcium hydroxide in concrete* (pp. 113–129).

McPolin, D., Basheer, P. A. M., Long, A. E., Grattan, K., & Sun, T. (2007). New test method to obtain pH profiles due to carbonation of concretes containing supplementary cementitious materials. *Journal of Materials in Civil Engineering, 19*(11), 936–946.

Mohammed, T. U., Hamada, H., & Yamaji, T. (2004). Concrete after 30 years of exposure – Part II: Chloride ingress and corrosion of steel bars. *ACI Materials Journal, 101*(1), 13–18.

Moradian, M., Shekarchi, M., Aabdollah, M., & Alidadi, R. (2012). Assessment of long-term performance of a 50-year-old jetty in the south of Iran. *Journal of Performance of Constructed Facilities, 26*(5), 633–643.

Moreno, M., Morris, W., Alvarez, M., & Duffó, G. (2004). Corrosion of reinforcing steel in simulated concrete pore solutions: Effect of carbonation and chloride content. *Corrosion Science, 46*(11), 2681–2699.

Neville, A. M. (2011). *Properties of concrete* (5th ed.). Harlow, England: Pearson Education Limited.

Ngala, V. T., & Page, C. L. (1997). Effects of carbonation on pore structure and diffusional properties of hydrated cement pastes. *Cement and Concrete Research, 27*(7), 995–1007.

Nielsen, E. P., Herfort, D., & Geiker, M. R. (2005). Binding of chloride and alkalis in Portland cement systems. *Cement and Concrete Research, 35*(1), 117–123.

Nolan, E. (1996). *Influence of near surface moisture gradients in concrete on Autoclam permeation measurements*. Queen's University Belfast.

Pakawat, S., & Uomoto, T. (2005). Effect of cyclic exposure of carbonation and chloride on corrosion of reinforcing steel in concrete. *Seisan Kenkyu, 57*(2), 29–32.

Papadakis, V. G. (2000). Effect of supplementary cementing materials on concrete resistance against carbonation and chloride ingress. *Cement and Concrete Research, 30*(2), 291–299.

Papadakis, V. G., Vayenas, C. G., & Fardis, M. N. (1991). Experimental investigation and mathematical modeling of the concrete carbonation problem. *Chemical Engineering Science, 46*(5), 1333–1338.

Parrott, L. J. (1991). Measurement of air permeability and relative humidity in cover concrete, *British Cement Association Report*, pp. 12.

RILEM. (2002). 178-TMC, Testing and modelling chloride penetration in concrete: Analysis of total chloride content in concrete. *Materials and Structures, 35*, 583–585.

Russell, D. P. (1999). *Influence of environmental conditions and material properties on carbonation in concrete*. Queen's University Belfast.

Russell, D., Basheer, P., Rankin, G., & Long, A. (2001). Effect of relative humidity and air permeability on prediction of the rate of carbonation of concrete. *Proceedings of the Institution of Civil Engineering – Structures and Buildings, 146*(3), 319–326.

Sagüés, A. A., Moreno, E., & Andrade, C. (1997). Evolution of pH during in-situ leaching in small concrete cavities. *Cement and Concrete Research, 27*(11), 1747–1759.

Sandberg, P. (1999). Studies of chloride binding in concrete exposed in a marine environment. *Cement and Concrete Research, 29*(4), 473–477.

Sisomphon, K., & Franke, L. (2007). Carbonation rates of concretes containing high volume of pozzolanic materials. *Cement and Concrete Research, 37*(12), 1647–1653.

Song, Y. D., Liu, J. H., Yi, F. X., Xu, B., & Ge, P. (2013). Research on the concrete performance in the marine environment. *Applied Mechanics and Materials, 345*, 184–188.

Suryavanshi, A., & Narayan Swamy, R. (1996). Stability of Friedel's salt in carbonated concrete structural elements. *Cement and Concrete Research, 26*(5), 729–741.

Tang, L. P. (2008). Engineering expression of the ClinConc model for prediction of free and total chloride ingress in submerged marine concrete. *Cement and Concrete Research, 38*(8–9), 1092–1097.

Tang, L. P., & Gulikers, J. (2007). On the mathematics of time-dependent apparent chloride diffusion coefficient in concrete. *Cement and Concrete Research, 37*(4), 589–595.

Xu, C., Wang, C. K., & Jin, W. L. (2011). Interaction effect of chloride attack and carbonation in concrete. *Journal of Building Materials, 14*(3), 376–380.

Zhao, H., Zhang, Y. M., & Ming, J. (2013). Tests and evaluation of structural concrete durability at Ningbo Marine wharf. *Hydro-Science and Engineering, 5*, 54–60.